

Proceedings World Geothermal Congress 2010

➤ [Table of Contents](#)

➤ [Author List](#)

➤ [Search this CD](#)

Convener:



International
Geothermal Association (IGA)

Co-Convenor:



Indonesian
Geothermal Association (INAGA)

Endorsed by:



Ministry of Energy & Mineral Resources
of the Republic of Indonesia

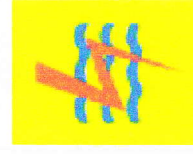
- [Technical Programme Committee](#)

- [Editorial Teams](#)

Sponsor Links:



PERTAMINA
GEOTHERMAL ENERGY



PT PLN (Persero)

HALLIBURTON

WGC2010 Technical Programme Committee

Cochairs: Roland N. Horne and Nenny Saptadji

Topic	Editors
1. Country Updates	John Lund Ruggero Bertani
2. Environmental and Societal Aspects	Regina Pascual Iwan Azof Fahmi H. Dereinda Katherine Luketina Jim Lawless
3. Legal and Regulatory Aspects	Fernando Echavarria Alimin Gintang Anton S. Wahjosoedibjo Maritje Hutapea
4. Economics and Financing	Dan Hoyer Christian Boissavy Suroto
5. Sustainability	Ladsi Rybach Benedikt Steingrimsson Gudni Axelsson
6. Case Histories	Steven Bjornstad Miklos Antics Alfonso Garcia-Gutierrez Colin Harvey Hadianto
7. Energy Pricing and Policies	Horst Kreuter Ali Ashat Asclepias Rahmi
8. Business Strategies	Madjedi Hasan
9. Geothermal Education	Nenny Saptadji Sachio Ehara
11. Exploration	Fausto Batini Marshall Reed Manny Ogena Asnawir Nasution Novi Ganefianto Ninik Suryantini Joel Renner Joel Ronne Jeff Witter
12. Geology	Susan Juch Lutz David Bruhn Luis Gutierrez-Negrin Sylvia Ramos Pri Utami Jufi Hadi James Stimac Anthony Budd Jim Lawless

13. Geophysics	Frank Horowitz Kasumi Yasukawa Lauro F. Bayrante Peter Leary Bill Cumming Imam B. Raharjo Mohammad Rachmat Sule Yunus Daud Greg Nordquist Tsuneo Ishido
14. Geochemistry	Tom Powell Mahendra P. Verma Francis Edward B. Bayon Adam Porowski <i>Rina Herdianita</i> Nilgün Güleç Brian Koenig Jim Lawless
15. Hydrogeology	Paul Brophy Adriano C. Cabel <i>Jan Dowgiallo</i> Ken Williamson Juliet Newson
16. Resource Assessment	Hideshi Kaieda Sachihiro Taguchi Toshiyuki Tosha Shiro Tamanyu
21. Drilling and Completion Technology	Paul Williams Stephen Pye Douglas Blankenship Andang Kustamsi Umrans Serpen
22. Reservoir Engineering	Roland Horne Mike Timlin Roland Horne Cedric Malate Steve Eneedy Ontowiryo Alamsyah Abdurrahman Satman Juliet Newson Mustafa Onur Hiroyuki Tokita
23. Injection Technology	Benedikt Steingrímsson Doddy Abdassah Niyazi Aksoy
24. Field Management	Dick Benoit Paul Moya Peter Barnett Mineyuki Hanano

25. Production Engineering and Steam Gathering Systems	Jim Lovekin Ronald Brooks Khasani
26. Power Generation	Thomas McAuliffe Shigeto Yamada T.A. Fauzi Soelaiman Ron DiPippo Mawardi Agani Ken Phair
27. Corrosion and Scaling	Oleh Weres Gestur Gíslason Ahmad Taufik Keith Lichti Norio Yanagisawa
28. Direct Use	Dornadula Chandrasekharam Taufan Surana Toni Boyd
29. Geothermal Heat Pumps	Iñaki Etxebarria Lekanda Hikari Fujii Tomoyuki Ohtani Hiroshi Asanuma Yuichi Niibori
31. EGS - Enhanced Geothermal Systems	Peter Ledingham Graeme Beardsmore Ann Robertson-Tait Pete Rose Hiroaki Niitsuma Isao Matsunaga Jim Lawless
32. Software for Geothermal Applications	Errol Anderson Sutopo Jericho Reyes Ryuichi Itoi
33. Health, Tourism and Balneology	Susan Hodgson Rosa María Prol-Ledesma
34. District Heating and Agriculture	Thorkell Erlingsson Jatmiko P. Atmodjo Toni Boyd
35. Clean Development Mechanism	Jim Randle
36. Geothermal Hydrogen Technology	Noriyoshi Tsuchiya
37. Advanced Technology	John Garnish Yasuhiro Fujimitsu
38. Integrated Energy Systems, Cascaded Uses	Sanja Popovska V. Sayogi Sudarman
39. Iceland Deep Drilling Project	Guðmundur Friðleifsson
40. Other	Kewen Li

WGC2010 Technical Programme

Topic

0. Keynotes
1. Country Updates
2. Environmental and Societal Aspects
3. Legal and Regulatory Aspects
4. Economics and Financing
5. Sustainability
6. Case Histories
7. Energy Pricing and Policies
8. Business Strategies
9. Geothermal Education
11. Exploration
12. Geology
13. Geophysics
14. Geochemistry
15. Hydrogeology
16. Resource Assessment
21. Drilling and Completion Technology
22. Reservoir Engineering
23. Injection Technology
24. Field Management
25. Production Engineering and Steam Gathering Systems
26. Power Generation
27. Corrosion and Scaling
28. Direct Use
29. Geothermal Heat Pumps
31. EGS - Enhanced Geothermal Systems (Hot Dry Rock)
32. Software for Geothermal Applications
33. Health, Tourism and Balneology
34. District Heating and Agriculture
35. Clean Development Mechanism
37. Advanced Technology and Hydrogen
38. Integrated Energy Systems, Cascaded Uses
39. Iceland Deep Drilling Project

13. Geophysics

Paper Number	Title	Authors
<u>1301</u>	<u>Integrated Geophysical Study of Lake Bogoria Basin, Kenya: Implications for Geothermal Energy Prospecting</u>	<u>Josphat Mulwa, Justus Barongo, Derek Fairhead, Nicholas Mariita and Jayanti Patel</u>
<u>1302</u>	<u>Calculation of the Maximum Effect of Deep Lakes on Temperature Measurements: Some Estimation Derived From the Geothermal Gradient Determination</u>	<u>Veniamin T. Balobaev, Izzy M. Kutasov and Lev V. Eppelbaum</u>
<u>1303</u>	<u>Physical Characteristic of Pong Kum Hot Spring, Chiang Mai, Thailand, Using Ground Geophysical Investigation</u>	<u>Neawsuparp K, Soisa T and Charusiri P</u>
<u>1304</u>	<u>Indirect Electromagnetic Geothermometer: Methodology and Case Study</u>	<u>Viacheslav V. Spichak and Olga K. Zakharova</u>
<u>1305</u>	<u>A Geophysical Characteristic Over Kelud Caldera Post November 2007 Eruption</u>	<u>Imam Suyanto, Sintia Windhi, and Wahyudi</u>
<u>1307</u>	<u>Numerical Modeling of Some Geothermal Sources in Gradient Media</u>	<u>Simeon Kostyanov and Velislav Stoyanov</u>
<u>1308</u>	<u>Heat Flow of Central Asia</u>	<u>Raisa P. Dorofeeva and Svetlana V. Lysak</u>
<u>1309</u>	<u>Integrated Geophysical Surveys to Characterize Tendaho Geothermal Field in North Eastern Ethiopia</u>	<u>Yohannes Lemma, Aklilu Hailu, Mohammednur Desissa, Ulrich Kalberkamp</u>
<u>1310</u>	<u>Interpreted Fracture Anomalies: Joint Imaging of Geophysical Signals from Fluid-Filled Fracture Zones in Geothermal Fields</u>	<u>Stephen Onacha, Eylon Shalev, Peter Malin, Peter Leary and Lake Bookman</u>
<u>1311</u>	<u>Controlled Source Magnetotelluric Survey of Mabini Geothermal Prospect, Mabini, Batangas, Philippines</u>	<u>Rogelio A. Del Rosario, Jr. and Alejandro F. Oanes</u>
<u>1312</u>	<u>Analysis of Spatial and Temporal Evolution of the Ground Deformation in the Cerro Prieto Geothermal Field (Mexicali Valley, B.C., Mexico) Using DInSAR and Leveling Data.</u>	<u>Olga Sarychikhina, Robert Mellors and Ewa Glowacka</u>
<u>1313</u>	<u>Hydrothermal System Beneath Usu Volcano Inferred from Self-potential Observation and Numerical Simulation</u>	<u>Hideaki Hase, Takeshi Hashimoto, Yasunori Nishida, Mitsuru Utsugi, Hiroyuki Inoue, and Mizue Saba</u>
<u>1314</u>	<u>The Resistivity Model of the Mindanao Geothermal</u>	<u>Carlos F. Los Baños,</u>

- Project, South Central Mindanao, Philippines
- 1315 Magnetotelluric Survey of NW Sabalan Geothermal Project, Iran
David M. Rigor, Jr., Domingo B. Layugan and Lauro F. Bayrante
Soheil Porkhial, David M. Rigor, Jr., Lauro F. Bayrante and Domingo B. Layugan
- 1316 3D Seismic Surveys and Deep Target Detection in the Larderello-Travale Geothermal Field (Italy)
Michele Casini, Simonetta Ciuffi, Adolfo Fiordelisi and Alfredo Mazzotti
- 1318 Geophysical Inversion of 3D Seismic Data in Panax's Limestone Coast Geothermal Project to Determine Reservoir Porosity
Margarita A. Pavlova and Ian Reid
- 1319 Micro-seismicity at the Miravalles Geothermal Field, Costa Rica (1994-2009): A Tool to Confirm the Real Extent of the Reservoir
Paul Moya and Waldo Taylor
- 1320 Reservoir Monitoring Using Hybrid Micro-Gravity Measurements in the Takigami Geothermal Field, Central Kyushu, Japan
Jun Nishijima, Hakim Saibi, Yayan Sofyan, Sachio Shimose, Yasuhiro Fujimitsu, Sachio Ehara, Yoichi Fukuda, Takashi Hasegawa and Makoto Taniguchi
- 1322 Effects of Pressure, Temperature, Fluid-Rock Interactions, and Phase Changes on the Physical Properties of Geothermal Reservoir Rocks: the Experimental Perspective
Harald Milsch, Erik Spangenberg, Siegfried Raab, Ansgar Schepers, Guido Blöcher, David Bruhn, Lúney H. Kristinsdóttir, Ólafur G. Flóvenz and Ernst Huenges
- 1324 Joint Inversion of VES and TEM Data for Investigation of Geothermal Resources and Sea Water Intrusion at Hammam Mousa Hot Spring, Sinai, Egypt
Gad El-Qady, Usama Massoud, Fernando Santos, El-Said Ragab, and Sultan Awad
- 1325 Geophysical Surveys for Geothermal Investigation in Central Poland
Wiesław Bujakowski, Antoni Barbacki, Barbara Czerwińska, Leszek Pajak, Marcin Pussak, Michał Stefaniuk, Zygmunt Trześniowski

- | | | |
|------|---|---|
| 1327 | <u>Advanced Technique for Reservoir Thermal Properties Determination and Pore Space Characterization</u> | <u>Yuri Popov, Dmitriy Miklashevskiy, Raisa Romushkevich, Sergey Safonov, Sergey Novikov</u> |
| 1328 | <u>Seismic Reflection Data and Conceptual Models for Geothermal Development in Nevada</u> | <u>Glenn Melosh, William Cumming, John Casteel, Kim Niggemann and Brian Fairbank</u> |
| 1329 | <u>Preprocessing for Reservoir Seismicity Location: Rotokawa Geothermal Field, New Zealand</u> | <u>Stephen Bannister, Steve Sherburn, Sandra Bourguignon, Stefano Parolai, Deborah Bowyer</u> |
| 1330 | <u>Horizontal Derivative from Gravity Data as a Tool for Drilling Target Guide in Wayang Windu Geothermal Field, Indonesia</u> | <u>Yudi Indra Kusumah, Suryantini, Hendro H., Wibowo.</u> |
| 1331 | <u>The Portable Electronic Divided Bar (PEDB): a Tool for Measuring Thermal Conductivity of Rock Samples</u> | <u>Anson M. Antriasian</u> |
| 1332 | <u>Magneto-telluric (MT) surveys in a challenging environment at Lihir Island, PNG</u> | <u>Greg Ussher, Jacques Charroy, Jose (Jun) Seastres and Gener Villafuerte</u> |
| 1335 | <u>Sustainable Geothermal Utilization Deduced from Mass Balance Estimation - A Case Study of Kamojang Geothermal Field, Indonesia-</u> | <u>Yayan Sofyan, Yunus Daud, Yustin Kamah and Sachio Ehara</u> |
| 1336 | <u>Discriminating Alteration of Pyroclastic Flow Deposits in an Active Volcano by SAR Image Analysis for Assessing the Geothermal System</u> | <u>Asep Saepuloh and Katsuaki Koike</u> |
| 1339 | <u>Kamchatkan Valley of the Geysers: Geodynamic Processes, Seismicity, Landsliding</u> | <u>Yu. Kugaenko, V. Saltykov</u> |
| 1340 | <u>Imaging of Geothermal Fluid Flow by Using Fluid Flow Electromagnetic Method</u> | <u>Hideki Mizunaga and Toshiaki Tanaka</u> |
| 1341 | <u>Seismic Emission in Geothermal Areas: Connection with Regional Seismicity</u> | <u>Vadim Saltykov</u> |
| 1342 | <u>Magnetotelluric exploration of the Gross Schönebeck</u> | <u>Gerard Muñoz, Oliver Ritter, Inga Moeck</u> |
| 1343 | <u>Specific Characteristics of the Gravity Aanalysis Within the Ulubelu Geothermal System Tanggamus, Lampung Indonesia</u> | <u>A. Hidayatika, S. Soengkono, Suharno and M. Särkowi</u> |
| 1344 | <u>Magnetic Analysis to Determine the Permeability of a Geothermal Reservoir: Case Study of the Mt. Rajabasa Geothermal System, Lampung Selatan Indonesia</u> | <u>Suharno, S. Soengkono and A. Hidayatika</u> |

- | | | |
|------|---|--|
| 1345 | <u>Seismic Tomography and Long-Period Earthquakes Observation and Modelling at the Hengill Geothermal Volcanic Complex, Iceland</u> | <u>Philippe Jousset,</u>
<u>Christian Haberland,</u>
<u>Klaus Bauer, Knutur Arnason, Michael Weber, Hubert Fabriol</u>
<u>Hermann Buness,</u>
<u>Hartwig von Hartmann,</u>
<u>Hanna-Maria Rumpel,</u>
<u>Thies Beilecke, Patrick Musmann, Rüdiger Schulz</u> |
| 1346 | <u>Seismic Exploration of Deep Hydrogeothermal Reservoirs in Germany</u> | <u>Okan Tezel, Hakan Hosgormez, Hakan Alp</u>
<u>Hartwig von Hartmann,</u>
<u>Hanna-Maria Rumpel,</u>
<u>Patrick Musmann,</u>
<u>Hermann Buness,</u>
<u>Charlotte Krawczyk,</u>
<u>Rüdiger Schulz</u> |
| 1347 | <u>The Time Domain IP Method In Geothermal Exploration: Balikesir(Gure) In Turkey</u> | <u>Svanbjörg Helga Haraldsdóttir, Hjalti Franzson, Knútur Árnason, Gunnlaugur M. Einarsson and Hédinn Björnsson</u> |
| 1348 | <u>Enhancing Hydrogeothermal Reservoir Detection by Seismic Imaging and Attributes</u> | <u>Ragna Karlsdottir and Olafur G Flovenz</u>
<u>Hjálmar Eysteinnsson,</u>
<u>Andemariam Teklesenbet, Guðni Karl Rosenkjær and Ragna Karlsdottir</u>
<u>Catherine Lewis Kenedi,</u>
<u>Eylon Shalev, Alan Lucas, and Peter Malin</u> |
| 1349 | <u>Comparison of Down-Hole and Surface Resistivity Data from the Hellisheidi Geothermal Field, SW-Iceland</u> | <u>Pedro A. Santos</u> |
| 1350 | <u>How the Use of Tem Changed the Resistivity Model of Oxarfjordur Temperature Field from an Earlier Dc Survey - a Case History</u> | <u>Dagoberto Herrera Cabezas</u>
<u>Ulrich Kalberkamp,</u>
<u>Gerlinde Schaumann,</u>
<u>Paul B. Ndonde, Sudian A. Chiragwile, Jonas M.</u> |
| 1351 | <u>Resistivity Survey in the Alid Geothermal Area, Eritrea, a Joint Interpretation of TEM and MT Data</u> | <u>Ulrich Kalberkamp,</u>
<u>Gerlinde Schaumann,</u>
<u>Paul B. Ndonde, Sudian A. Chiragwile, Jonas M.</u> |
| 1352 | <u>Microseismicity and 3-D Mapping of an Active Geothermal Field, Kilauea Lower East Rift Zone, Puna, Hawaii</u> | <u>Ulrich Kalberkamp,</u>
<u>Gerlinde Schaumann,</u>
<u>Paul B. Ndonde, Sudian A. Chiragwile, Jonas M.</u> |
| 1353 | <u>Contribution of Magneto-Telluric Method to Geothermal Development in El Salvador</u> | <u>Ulrich Kalberkamp,</u>
<u>Gerlinde Schaumann,</u>
<u>Paul B. Ndonde, Sudian A. Chiragwile, Jonas M.</u> |
| 1354 | <u>Precision Gravity Data of the Miravalles Geothermal Field an Ongoing Assessment.</u> | <u>Ulrich Kalberkamp,</u>
<u>Gerlinde Schaumann,</u>
<u>Paul B. Ndonde, Sudian A. Chiragwile, Jonas M.</u> |
| 1355 | <u>Surface Exploration of a Viable Geothermal Resource in Mbeya Area, SW Tanzania. Part III: Geophysics</u> | <u>Ulrich Kalberkamp,</u>
<u>Gerlinde Schaumann,</u>
<u>Paul B. Ndonde, Sudian A. Chiragwile, Jonas M.</u> |

- 1357 Seismic Attribute Analysis of the 3-D Depth-Migrated Image and Its Correlation with the Induced Microseismicity
Mwano
Jaya, M. S., Buske, S., Kummerow, J., Reshetnikov, A. and Shapiro, S.
- 1358 Temperature-Dependent Seismic Properties of Geothermal Core Samples at In-Situ Reservoir Conditions
Jaya, M. S., Shapiro, S., Kristindóttir, L., Bruhn, D., Milsch, H. and Spangenberg, E
- 1360 Determination of Negative Density Changes in the Kamojang Geothermal Field Using Time-Lapse Microgravity Analysis
Ahmad Zaenudin, Wawan G.A. Kadir, Djoko Santoso, Doddy Abdassah, and Yustin Kamah ✓
- 1361 Magnetotelluric Static Shift Correction Using Time Domain Electromagnetics Case Study Indonesian Geothermal Rough Fields
Riki Irfan, Yustin Kamah, Eddy Gaffar, Ts Winarso
- 1362 The First Magnetotelluric Investigation of the Tawau Geothermal Prospect, Sabah, Malaysia
Yunus Daud, Fredolin Javino, Mohd. Nawawi Mohd. Nordin, Mohd. Razak, Ibrahim Amnan, Rahman Saputra, Lendriadi Agung, Sucandra
- 1363 Monitoring of Microearthquakes and Acoustic Emissions Within the Hengill-Hellisheidi Geothermal Reservoirs, June-August 2007
Anastasia W. Wanjohi
- 1364 Electrical resistivity at the Travale geothermal field (Italy)
Adele Manzella, Carlo Ungarelli, Giovanni Ruggieri, Chiara Giolito and Adolfo Fiordelisi
- 1365 Characterization of Temporal Change of Deep Resistivity around Geothermal Reservoir Using Magnetotelluric Survey
Asaue, H., Kubo, T., Yoshinaga, T. and Koike, K.
- 1366 Seismic Exploration Around the Geothermal Research Well Gross Schoenebeck (NE German Basin) Combining Tomographic and Reflection Seismic Methods
Klaus Bauer, Inga Moeck, Ben Norden, Bianca Kallenberg, Albrecht Schulze and Michael Weber
- 1367 Seismic and Electromagnetic Study of Reservoir Properties for Geothermal Applications
Michele Pipan, Emanuele Forte, Anna Del Ben, Hugo Fernando Navas Alonzo, Geoffrey Giudetti,

- | | | |
|------|---|---|
| 1371 | <u>Resistivity Structures of Lahendong and Kamojang Geothermal Systems Revealed from 3-D Magnetotelluric Inversions, A Comparative Study</u> | <u>Supriyanto Suparno</u>
<u>Imam B. Raharjo,</u>
<u>Virginia Maris, Philip E.</u>
<u>Wannamaker, David S.</u>
<u>Chapman</u> |
| 1374 | <u>Interpretation of DC Resistivity Data to Recognized Geothermal Prospect at Sampuraga, North Sumatera, Indonesia</u> | <u>Asep Sugianto and</u>
<u>Bakrun</u> |
| 1375 | <u>Interpretation of Subsurface Geological Structure of Massepe Geothermal Area Using Resistivity Data</u> | <u>Ahmad Zarkasyi and</u>
<u>Yuanno Rezky</u> |
| 1377 | <u>New Interpretation of DC Resistivity Data in the Sibayak Geothermal Field, Indonesia</u> | <u>Supriyanto Suparno,</u>
<u>Yunus Daud, Syamsu</u>
<u>Rosid, Dede Djuhana</u>
<u>and Yayan Sofyan</u> |
| 1378 | <u>Precision Gravity Modeling and Interpretation at the Salak Geothermal Field, Indonesia</u> | <u>Gregg A. Nordquist,</u>
<u>Jorge Acuña and Jim</u>
<u>Stimac</u> |
| 1379 | <u>Monitoring Microseismicity during Well Stimulation at the Salak Geothermal Field, Indonesia</u> | <u>Djoko Anityo S.</u>
<u>Wibowo, Gregg A.</u>
<u>Nordquist, Jim Stimac</u>
<u>and Auardi Suminar</u> |
| 1380 | <u>Hot Springs and Underwater Crater EM Sounding and DC Tomography</u> | <u>Yuri Manstein, Gregory</u>
<u>Panin, Dmitry Kuzmin</u> |
| 1382 | <u>Three-Dimensional Interpretation of AMT Data in Ogiri Geothermal Field, Japan</u> | <u>Toshihiro Uchida</u> |
| 1385 | <u>Self-Potential Monitoring with Reservoir Simulation in a Geothermal Field, Japan</u> | <u>Toshiyuki Tosha,</u>
<u>Tsuneo Ishido, and</u>
<u>Mituhiko Sugihara</u> |
| 1386 | <u>Magnetotelluric Experiments in the Aliaga Geothermal Field, Western Turkey</u> | <u>Cemal Kaya and Ahmet</u>
<u>T. Basokur</u> |
| 1387 | <u>A Multi-Parameter Measurement System at Koseto (Shizuoka, Japan) and Its Responses During the Large Earthquakes Since 2003</u> | <u>Ömer Aydan, Hisataka</u>
<u>Tano and Yoshimi Ohta</u> |
| 1388 | <u>Characterizing a Geothermal Reservoir Using Broadband 2-D MT Survey in Theistareykir, Iceland</u> | <u>Gang Yu, Árni</u>
<u>Gunnarsson, Zhanxiang</u>
<u>He, and Helga Tulinius</u> |
| 1389 | <u>An On-Line Monitoring System of Multi-Parameter Changes of Geothermal Systems Related to Earthquake Activity in Western Anatolia in Turkey</u> | <u>Halil Kumsar, Ömer</u>
<u>Aydan, Hisataka Tano,</u>
<u>Reşat Ulusay, Sefer B.</u>
<u>Celik, Mustafa Kaya</u>
<u>and Muhittin Karaman</u> |
| 1390 | <u>2-D Magnetotellurics and Gravity at the Geothermal Site at Soultz-sous-Forêts</u> | <u>Eva Schill, Johannes</u>
<u>Geiermann, Jessica</u> |

Characterization of Negative Density Contrast in the Mounting Creek and Ball Lake Basins

- | | | |
|-------------------------------------|--|---|
| <p>1392</p> <p>1396</p> <p>1399</p> | <p><u>3D Geological Modelling of Potential Geothermal Energy Reservoirs in the Flinders Ranges, Australia</u></p> <p><u>Resistivity Imaging of Geothermal Resources Using 1D, 2D and 3D MT Inversion and TDEM Static Shift Correction Illustrated by a Glass Mountain Case History</u></p> <p><u>Structural Significance of the Results of a Resistivity study in Alid Geothermal Area</u></p> | <p><u>Kümmritz</u></p> <p><u>Guillaume Backé, David Giles, Graham Baines, and Kathryn Amos</u></p> <p><u>William Cumming and Randall Mackie</u></p> <p><u>Ermias Yohannes</u></p> |
|-------------------------------------|--|---|

Three-dimensional geological models of the Flinders Ranges and Mounting Creek and Ball Lake basins were constructed using data from a series of seismic surveys. The models were used to estimate the potential geothermal energy resources in the basins. The models were also used to estimate the potential geothermal energy resources in the basins. The models were also used to estimate the potential geothermal energy resources in the basins.

The results of the resistivity study in the Alid Geothermal Area are presented in this paper. The results show that the resistivity is high in the area, which is consistent with the presence of a geothermal system. The results also show that the resistivity is low in the area, which is consistent with the presence of a geothermal system.

1. INTRODUCTION

The purpose of this study is to provide a detailed description of the geology and geophysics of the Alid Geothermal Area. The study is based on a series of seismic surveys and resistivity data. The results of the study are presented in this paper.

The results of the resistivity study in the Alid Geothermal Area are presented in this paper. The results show that the resistivity is high in the area, which is consistent with the presence of a geothermal system. The results also show that the resistivity is low in the area, which is consistent with the presence of a geothermal system.

The results of the resistivity study in the Alid Geothermal Area are presented in this paper. The results show that the resistivity is high in the area, which is consistent with the presence of a geothermal system. The results also show that the resistivity is low in the area, which is consistent with the presence of a geothermal system.

The results of the resistivity study in the Alid Geothermal Area are presented in this paper. The results show that the resistivity is high in the area, which is consistent with the presence of a geothermal system. The results also show that the resistivity is low in the area, which is consistent with the presence of a geothermal system.

2. STUDY AREA

The study area is located in the Alid Geothermal Area. The area is characterized by a series of faults and a high degree of seismicity. The results of the study are presented in this paper.

The results of the resistivity study in the Alid Geothermal Area are presented in this paper. The results show that the resistivity is high in the area, which is consistent with the presence of a geothermal system. The results also show that the resistivity is low in the area, which is consistent with the presence of a geothermal system.

3. DATA

The data used in this study are presented in this paper. The data include seismic data and resistivity data. The results of the study are presented in this paper.

The results of the resistivity study in the Alid Geothermal Area are presented in this paper. The results show that the resistivity is high in the area, which is consistent with the presence of a geothermal system. The results also show that the resistivity is low in the area, which is consistent with the presence of a geothermal system.

$$\rho = \frac{1}{\sigma} = \frac{1}{\frac{1}{\rho_1} + \frac{1}{\rho_2} + \dots + \frac{1}{\rho_n}}$$

The results of the resistivity study in the Alid Geothermal Area are presented in this paper. The results show that the resistivity is high in the area, which is consistent with the presence of a geothermal system. The results also show that the resistivity is low in the area, which is consistent with the presence of a geothermal system.

$$\rho = \frac{1}{\sigma} = \frac{1}{\frac{1}{\rho_1} + \frac{1}{\rho_2} + \dots + \frac{1}{\rho_n}}$$

The results of the resistivity study in the Alid Geothermal Area are presented in this paper. The results show that the resistivity is high in the area, which is consistent with the presence of a geothermal system. The results also show that the resistivity is low in the area, which is consistent with the presence of a geothermal system.

$$\rho = \frac{1}{\sigma} = \frac{1}{\frac{1}{\rho_1} + \frac{1}{\rho_2} + \dots + \frac{1}{\rho_n}}$$

where

$$\rho = \frac{1}{\sigma} = \frac{1}{\frac{1}{\rho_1} + \frac{1}{\rho_2} + \dots + \frac{1}{\rho_n}}$$

The results of the resistivity study in the Alid Geothermal Area are presented in this paper. The results show that the resistivity is high in the area, which is consistent with the presence of a geothermal system. The results also show that the resistivity is low in the area, which is consistent with the presence of a geothermal system.

Determination of Negative Density Changes in the Kamojang Geothermal Field Using Time-Lapse Microgravity Analysis

Ahmad Zaenudin¹, Wawan G.A. Kadir², Djoko Santoso², Doddy Abdassah², Yustin Kamah³

¹Physics Dept. Lampung University, ²FTTM ITB, ³Geothermal Energy Pertamina

zae_unila@yahoo.com

Keywords: time-lapse microgravity, stripping filter, density changes

ABSTRACT

Ground deformations and gravity changes were measured in order to study density distribution changes caused by the production and re-injection into the Kamojang geothermal reservoir. In the last two years (2006-2007) we conducted two elevation measurements, in July 2006 and July 2007. In addition, we carried out three microgravity surveys, in June 2006, November 2006 and July 2007. The gravity stations were located at 88 benchmarks to cover the survey area. From those three maps we have already made two time-lapse microgravity anomaly change maps, covering the periods of June-November 2006 and June 2006-July 2007.

Gravity effects due to density change in the reservoir (caused by production/re-injection) were obtained by correcting the measured gravity anomalies of the gravitational effect to vertical ground movements (subsidence) and ground water level changes. Gravity anomaly measured on the surface due to elevation change has a positive value for elevation lowering (subsidence) and the gravity change is approximately 3 μGal for 1 cm elevation change. Gravity anomaly related to dynamic groundwater was corrected by a stripping filter. By using inversion methods, a map of density distribution changes has been produced during this period.

1. INTRODUCTION

Applications of the gravity method are carried out for monitoring purposes. Multiple studies have been performed, for example for monitoring EOR at oil and gas fields (Santoso, et al, 2004; Hare, et al. 1999), and geothermal fields (Allis and Hunt, 1986; Fujimitsu et al, 2000). Gravity was also monitored in the Kamojang geothermal field. Results of time lapse gravity surveys for 5 periods (1984, 1988, 1992, and 1999) by Pertamina Geothermal indicate that the negative gravity anomaly from 1984 to 1999 is around -250 μGal at the center of production; whilst the subsidence maximum is at 0.2 m.

Gravity monitoring in geothermal fields is used to predict the distribution of density change in the reservoir and/or behavior of a two-phase zone as a result of production and reinjection of geothermal fluid. Gravity anomaly changes between two surveys result from changing ground surface and subsurface as well (Santoso, dkk, 2006). Changes of gravity in the subsurface are due to changing groundwater level, and saturation of fluid in reservoir. Therefore, the microgravity anomaly in the reservoir needs to be corrected to account for subsidence and lowering of groundwater level.

Corrected gravity due to subsidence can be done directly if elevation changes are known from leveling or GPS surveys.

Gravity corrections for groundwater level change can be done with the stripping filter method.

This paper analyzes the distribution of density changes in the Kamojang geothermal field using time-lapse microgravity anomaly period of June 2006 to July 2007. Modified filter stripping was used to separate gravity anomaly near surface (groundwater level) from that in the reservoir.

2. METHOD AND DATA

2.1 Time-Lapse Microgravity Survey and GPS

During period of 2006-2007, we conducted time lapse gravity surveys 3 times that were June 2006, November 2006 and July 2007, using a digital Lacoste & Romberg G-1158 gravimeter. The numbers of benchmarks used for the surveys were 88 with the same looping to get gravimeter drifts that were relatively similar. Tidal correction was measured directly by the Lacoste & Romberg G-508 gravimeter, which was read continuously at the base.

The elevation of 26 benchmarks was measured using GPS (Trimble 4000 LS) with measurement duration of 5-6 hours at every point.

Stripping Filter

To separate gravity anomalies from shallow-subsurface (groundwater level change) and deep (geothermal reservoir), we applied filter stripping, modified from Cordell (1985) and Aina (1994).

Gravity anomaly caused the mass density changes in the horizontal direction can be written as,

$$\Delta g(x, y, 0) = G\Delta\rho \int_{h_1}^{h_2} \int_{-\infty}^{\infty} \int_{-\infty}^{\infty} \frac{S(\alpha, \beta)\gamma}{[(x-\alpha)^2 + (y-\beta)^2 + (\gamma)^2]^{\frac{3}{2}}} d\alpha d\beta d\gamma. \quad (1)$$

If an anomaly observed on the surface stems from changes in the shallow-subsurface and the deep-subsurface, then the total anomaly can be written as,

$$g(x, y) = g_s(x, y) + g_d(x, y) \quad (2)$$

where subscripts s and d denote shallow and deep. Equations (1) and (2) in the wave number domain can be written:

$$G(u, v, 0) = \frac{8\pi K}{k.u.v} \Delta\rho \cdot \sin\left(\frac{au}{2}\right) \sin\left(\frac{bv}{2}\right) e^{-kh_1} [1 - e^{-k(h_2-h_1)}] \quad (3)$$

and

$$G(u, v) = G_s(u, v) + G_d(u, v) \quad (4)$$

where u is wave number coordinate, $G(u)$ is Fourier transform (TF) from $g(x)$, $G_s(u)$ is TF from $g_s(x)$, $G_d(u)$ is TF from $g_d(x)$, $t_s = h_{bs} - h_{ts}$ and $t_d = h_{bd} - h_{td}$ is prism thickness. The continuity equation (3) can be written for shallow and deep sources separately, i.e.:

$$G_s(u, v) = \frac{8\pi K}{k.u.v} \Delta\rho \sin\left(\frac{au}{2}\right) \sin\left(\frac{bv}{2}\right) e^{-kh_u} [1 - e^{-k(h_{ts} - h_{ts})}] \quad (5)$$

$$\text{and } G_d(u, v) = \frac{8\pi K}{k.u.v} \Delta\rho \sin\left(\frac{au}{2}\right) \sin\left(\frac{bv}{2}\right) e^{-kh_u} [1 - e^{-k(h_{td} - h_{td})}] \quad (6)$$

Equations (5) and (6) give an important basis design for the desired filter stripping. Filter stripping for a shallow anomaly spectrum can be written:

$$S(u, v) = \frac{1}{1 + \frac{G_d(u, v)}{G_s(u, v)}} \quad (7)$$

Substituting equations (5) and (6) to equation (7) is:

$$S(u, v) = \frac{1}{1 + \alpha\beta \left(\frac{u}{v}\right)^{\xi} e^{-k\xi}} \quad (8)$$

$$\text{where } \alpha = \frac{\Delta\rho_d}{\Delta\rho_s}, \beta = \frac{1 - e^{-h_d}}{1 - e^{-h_s}} \text{ dan } \xi = h_{th} - h_{ts}$$

Equation (8) is filter stripping which a form identical to the equation presented by Cordell (1985) and Aina (1994). Here α is comparison density, β thickness comparison (t) and ξ it is the difference in depth between the shallow and deep layers.

3. RESULTS AND DISCUSSION

3.1 Subsidence and Groundwater Level Changes in the Survey Area

To determine change of gravity, each gravity station collected data with high accuracy (leveling or GPS), i.e. on the order of mm. Figure 1 as measured by GPS in June 2006 and July 2007. Areas experiencing subsidence are parallel to the SW-NE direction with Citepus fault and Kendang fault. Maximum subsidence is 6 cm, which is the south part around the rim-structure. The largest inflation (6 cm) was measured in the North field. Transformation of gravity as result of subsidence every 1 cm is around 3,08 μGal .

Changes in groundwater level were calculated using local rainfall based on equation of Akasaka and Nakanishi (2000), as seen in Figure 2. The change in groundwater level for the period of June 2006 to November 2006 was -1,502 m; whilst during the period from June 2006 to July 2007 it was +0,396 m. Based on previous studies and measured ground water level from wells it is on average 5 to 10 m, and the depth of geothermal reservoir around 700 m (Kamah et al., 2005).

3.2 Time-lapse Microgravity Anomaly, Stripping Filter and Inversion

A survey monitoring gravity changes needs to be conducted with high accuracy. In addition, the survey must be done with similar sequence (looping) so that every gravity station in each period has the approximately equal drift. Tidal

correction was applied using measured tidal variations from the base. Three gravity observations were conducted to obtain two microgravity anomaly data sets from June '06 to November '06 and June '06 to July '07. Both microgravity anomalies are corrected to account for subsidence in each period. The result is an estimate of the change in distribution of density in the subsurface. The gravity anomaly in the subsurface consists of a shallow anomaly (groundwater level change) and a deep anomaly (change of distribution of geothermal reservoir density). These two anomalies were separated using filter stripping.

Filter stripping performed by multiplying the gravity subsurface spectrum with the filter spectrum built from shallow and deep layer parameters (groundwater level change). These were estimated from geological data, well data and other geophysical data. The filter stripping parameters are density change (α), thickness comparison (β) and depth difference (ξ) between the shallow layer and deep layer (Equation (8)). The results show a change of shallow layer density ($\Delta\rho_s$) 0,3 gr/cm³, deep layer density in ($\Delta\rho_d$) 0,018 gr/cm³; an average depth of 5m for the shallow layer and 700m for the deep layer (reservoir). Filter stripping minimizes the gravity effects of the shallow layer and maximizes the gravity effects of the deep layer. Microgravity anomaly changes in time, which result from changes in distribution density in the geothermal reservoirs, Figure 3 and Figure 4. These were obtained using the filter. The research area is dominated by negative gravity anomaly, with the maximum negative gravity anomaly located in the western and northern parts of the field. Figure 4 shows gravity change over a one year period, with negative gravity anomaly equal to -80 μGal .

The distribution of density change in the reservoir is found using inversion methods. A field model is built with 16 cells in the x-axis direction, 17 cells in the y-axis direction with a grid of 250 m x 250 m, and 9 cells in z-axis direction with 4 layers. Modeling was applied using the software Grav3D version 20 of UBC-GEOPHYSICAL Inversion Facility, University of British Columbia.

Figures 5 and 6 are maps of density change at a depth of 1100 m for the periods of June '06 to November '06 and June '06 to July '07.

CONCLUSION

Gravity monitoring at the Kamojang geothermal field has been carried out 5 times since the year 1984. In this study the change of gravity was measured over a period of one year, utilizing correction methods based on GPS data and the filter stripping method to separate gravity anomaly caused by shallow subsurface variations from deep reservoir variations. This way we could estimate the distribution of reservoir density using a data collected over a relatively short period.

The stripping filter can separate microgravity anomalies, as a result of reservoir mass decrease due to extraction of vapor and/or addition of reservoir mass from reinjection of geothermal brine, from gravity anomalies resulting from lowering of the water table. Subsidence (dry-out) is shown by negative microgravity time-lapse anomaly (-) and additional mass of injection water in the reservoir (recharge) is shown by positive microgravity time-lapse anomaly (+). Negative microgravity time-lapse anomaly (-) is interpreted as negative change in density anomaly (-) and positive microgravity time-lapse anomaly (+) is interpreted as positive change in density.

Filtering result shows that negative gravity anomaly is related to production wells. Based on time-lapse anomaly microgravity maps from the period of June 06 to July 07, negative concentration anomalies are located in the western field, i.e. around rim structures. This can be related to activity of production wells (KMJ-22, KMJ-28, KMJ-37, KMJ-41, KMJ-42, KMJ-27 and KMJ-65) in the area. Based on a 3D cross sectional map at depth of 1100 m (+400 m a.s.l.), this area is represented by negative density from -0.02 up to -0.04 gram/cm³. This also proves that injection amounts through injection well KMJ-35, and KMJ-46 in the area is not effective. Positive anomaly is represented by accumulation of injection water from injection well and or accumulation of water meteoric flowing through faults. Existence of fluid flow in the reservoir is clarified with results of analysis tracer injection and microearthquake (MEQ).

REFERENCES

- Aina, A. (1994) : A simple of Cordell's stripping filter, *Geophysics*, **59**, 488-490.
- Akasaka, C., dan Nakanishi, S. (2000) : A evaluation of the background noise for microgravity monitoring in the Oguni field, Japan, *Proceeding of 25th Stanford Geothermal Workshop*, 24-26 January 2000.
- Allis, R.G., Gettings, P., dan Chapman, D.S. (2000) : Precise gravimetry and geothermal reservoir management, *Proceedings Twenty-Fifth Workshop on Geothermal Reservoir Engineering*, Stanford University, Stanford California.
- Cordell, L. (1985) : A stripping filter for potential-field data, 55th Annual International Meeting, *SEG, Expanded Abstracts*, 217-218.
- Fujimitsu, Y., Nishijima, J., Shimosako, N., Ehara, S., dan Ikeda, K. (2000) : Reservoir Monitoring by Repeat Gravity Measurements at The Takigami Geothermal Field, Central Kyushu, Japan, *Proceeding World Geothermal Congress*, Kyushu-Tohoku, Japan, 573 – 577.
- Hare, J.L., Ferguson, J.F., Aiken, C.L.V., dan Bradly, J.L. (1999) : The 4-D microgravity methode for waterflood surveillance : a model study for the Prudoe Bay reservoir- Alaska', *Geophysics*, **64**, 78-87.
- Kamah, M.Y., Mutthalib, Negara, C., Silaban, MSP, Silitonga, T.H., Leonardus, A.M.N., Pulungan, I., dan Mufroil, H. (2000): *Laporan Survei Gravitasi Presisi Periode 99-00 Lapangan Produksi Panasbumi Kamojang, Jawa Barat*
- Kamah, M.Y., Dwikorianto, T., Zuhro, A.A., Sunaryo, D., dan Hasibuan, A. (2005) : The productive feed zones identified based on Spinner data and application in the reservoir potential review of Kamojang geothermal field area, Indonesia, *Proceeding WGC 2005*, Antalya, Turkey, 1-6.
- Santoso, D., Kadir., W.G.A., Sarkowi. M., Adriansyah, dan Waluyo, (2004) : Time-lapse microgravity study for injection water monitoring of Talang Jimar field, *Proceedings of the 7th SEGJ International Symposium*, Sendai-Japan 24-26 November 2004, 497-502.
- Santoso, D., Sarkowi, M., dan Kadir, W.G.A. (2006) : Determination of negatif ground water withdrawal in Semarang City area using time-lapse microgravity analysis, *Proceedings of the 7th SEGJ International Symposium*, Sendai-Japan 24-26 November 2004.

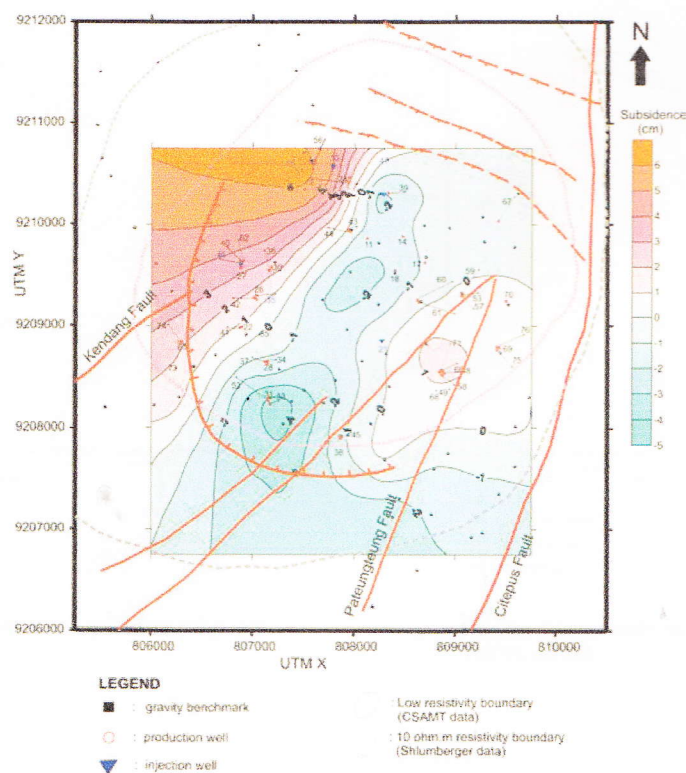


Figure:1 Subsidence rate in Kamojang 2006-2007

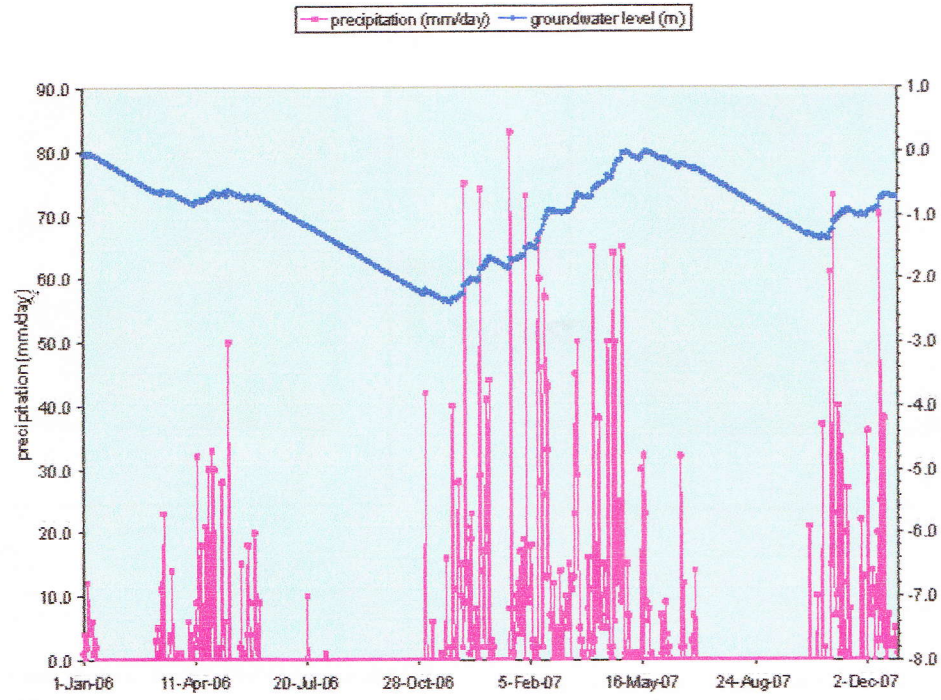


Figure 2: Groundwater level and precipitation

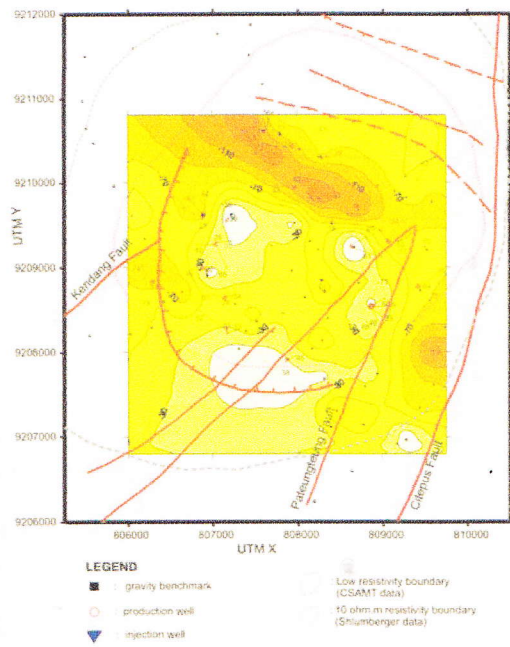


Figure 3: Gravity anomaly used stripping filter Jun'06-Nov'06 period

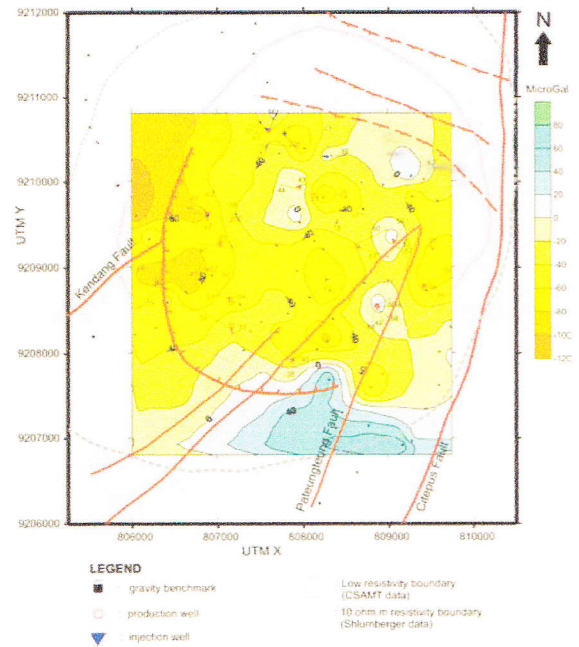


Figure 4: Gravity anomaly used stripping filter Jul'07-Jun'06 period



Figure 5: Density changes Jun'06-Nov'06 period at 1100 m depth

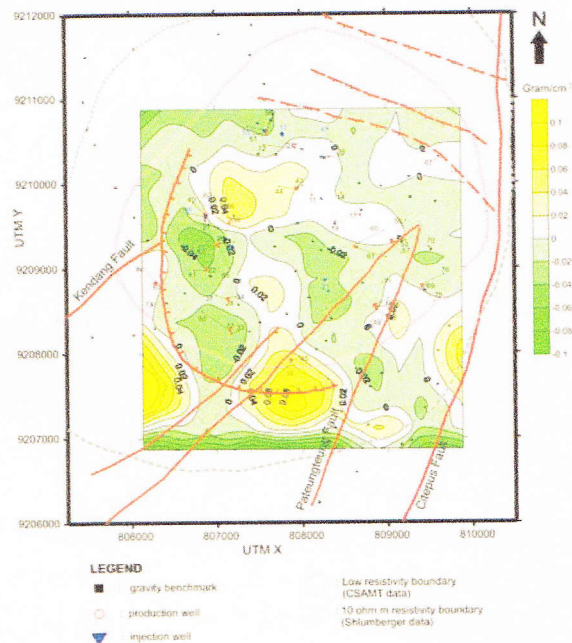


Figure 6: Density changes Jul'07-Jun'06 period at 1100 m depth